Typeset with jjap2.cls <ver.1.0> Regular Paper

High-frequency wireless-electrodeless QCM for immunosensors

Hirotsugu OGI, Kazuma MOTOHISA, Kenichi HATANAKA, Toshinobu OHMORI, Masahiko HIRAO, and Masayoshi NISHIYAMA[1]

Graduate School of Engineering Science, Osaka University, 1-3 Machikaneyama, Toyonaka, Osaka 560-8531, Japan
[1]Central Workshop, Osaka University Machikaneyama 1-2, Toyonaka, Osaka 560-8531, Japan

Wireless-electrodeless high-frequency quartz crystal microbalance (QCM) was developed for monitoring biochemical reactions in real time without using any labeling procedures. The analytical vibrational calculation for a multilayered plate showed that the QCM sensitivity significantly deteriorates when metallic electrodes are present on the crystal surfaces, indicating the importance of an electrodeless QCM biosensor. The 30-μm thick electrodeless QCM immunosensor was excited and its mechanical vibration was detected contactlessly by the antenna located outside the QCM cells. The homebuilt QCM system was used to detect human immunoglobulin G (hIgG) via staphylococcal protein A (SPA) immobilized on the crystal surface and to demonstrate higher sensitivity of the electrodeless QCM than that of the conventional QCM. The 30 μm thick QCM, showing 54 MHz fundamental frequency, successfully monitored the hIgG-SPA binding reaction for the hIgG concentration of 100 pg/mL.

KEYWORDS: QCM, biosensor, wireless, electrodeless

1. Introduction

Quartz crystal microbalance (QCM) has been intensively studied because of its two important roles. First, it can be used for the detection of specific protein markers that are excreted by corresponding disorders; for examples, glypican-3 for hepatocellular carcinoma[1)] and amyloid-β protein for Alzheimer disease.[2)] Early detection of these protein markers increases the possibility of their permanent cures. Second, a QCM biosensor involves ability of quantitative determination of the kinetic constants related with the biochemical reactions,[3,4)] resulting in the affinity between biomolecules, which highly contributes to the development of an effective antibody for a specific antigen, that is the drug discovery. Thus, the QCM technique has been applied to study various biochemical reactions including immunoglobulins,[4–6)] DNA,[7,8)] Dioxins,[9)] and so on.

The QCM biosensor realizes the real-time and labeling-free monitoring of biochemical reactions through the change of its mechanical resonance frequency. The target biomolecules are adsorbed by the receptor molecules immobilized on the QCM surface, resulting in the increase of the effective mass and decrease of the resonance frequency.[10)] The fractional frequency change, or the sensitivity, is governed by the thickness of the oscillator; thinner oscil-

lator causes larger amount of the frequency change when the target molecules are adsorbed. Therefore, developing a higher-sensitive QCM definitely requires a thinner quartz plate. However, electrodes deposited on the both surfaces have posed difficulties for making the thinner QCM. Owing to the high electric conductivity and high affinity to thiol reagents for making a self-assembled monolayer, gold layers have been deposited for the electrodes. However, the mass density of gold is much higher than that of alpha-quartz by a factor of 7.3 and such heavy metallic layers cause very large inertia resistance because the vibrational acceleration shows the maxima at the oscillator surfaces. Obviously, an electrodeless approach is expected to achieve an ultra-high sensitive QCM.

We have developed an isolated electrodeless oscillator using a stepped nickel rod[11] and applied it to a biosensor.[12] However, the stability of the resonance frequency was inadequate because of the larger temperature coefficient of the elastic constants of nickel. We then developed an isolated electrodeless QCM using a 0.3 mm AT-cut alpha-quartz.[13] The vibration of the crystal was generated and detected by the line antenna[14] located outside the cell, allowing the noncontacting measurement. This type of electrodeless QCM showed higher sensitivity than the conventional QCM and the nickel-rod oscillator. Here, we develop much more sensitive QCM system using an AT-cut alpha-quartz of 30-μm thick, whose fundamental resonance frequency is near 54 MHz. The human immunoglobulin G (hIgG) is detected by staphylococcal protein A (SPA) immobilized on the crystal surface. It clearly monitored their binding reaction in real time even when the hIgG concentration was as small as 100 pg/mL.

2. Contactless Frequency Measurement for Electrodeless QCM

Figure 1 shows the cross-sectional view of the homebuilt QCM cell. The 30-μm thick AT-cut quartz crystal is fixed by the silicon-robber sheets. The line antenna[13,14] is embedded in the bottom wall of the cell, which consists of three straight copper wires; one for generation, one for detection, and the other for grounding. The tone-bursts voltage is applied to the generation wire to induce the quasistatic electric field perpendicular to the antenna, which penetrates into the crystal and generates the pure shear wave propagating in the thickness direction of the crystal through the converse piezoelectric effect. After the excitation, the receiving wire detects the mechanical vibrations of the crystal through the piezoelectric effect.[15,16] The received signals are fed to the superheterodyne spectrometer to extract the amplitude and phase of the vibration at the same frequency component as the driving signal.[17] Thus, the crystal requires neither electrodes nor wiring on the oscillator surface, which we define as the wireless-electrodeless oscillator..

Scanning the driving frequency and acquiring the amplitude, the resonance spectrum is obtained and the Gaussian-function fitting gives the resonance frequency. We call this the frequency-scan method. Because the frequency-scan method required longer time ($\sim$10 s), after the resonance frequency became stable, we monitored the phase of the received signal at the

fixed frequency and determined the resonance-frequency change from the linear relationship between the phase and frequency near the resonance frequency. We call this the phase method.

3. Surface Modification

A 9-nm thick Au film was deposited after 1-nm thick Cr film on one side of the crystal for making the gold-thiol binding effective, not for an electrode. (Indeed, the 9-nm thick Au electrode hardly deteriorates the QCM sensitivity as seen later in Fig. 2.) The crystal was cleaned in the piranha solution (98%H_2SO_4:33%H_2O_2=4:1). After rinsing with ultrapure water, it was immersed in 50 μM 5-carboxy-1-pentanethiol/ethanol solution for 3 h. The surface was activated by 100 mM EDC (1-ethyl-3-(3-dimethylaminopropyl)carbodiimide, hydrochloride) solution and 100 mM sulfo-NHS (N-hydroxysulfosuccinimide sodium salt) solution. SPA was then immobilized on the surface by immersing the oscillator into the phosphate-buffer solution (PBS, pH 7.0) containing 1 mg/ml SPA for 24 h at 4 ° C. The remaining activated ester sites were blocked with a 10 mg/mL bovine serum albumin (BSA) solution.

hIgG was from Athens Research and Technology, Inc. (product num. 16-16-090707; purity ∼95%). SPA was from Zymed Laboratories, Inc. (product num. 10-1100; purity 98%). 5-carboxy-1-pentanethiol (product num. C387) and EDC (product num. W001) were from Dojindo Laboratories. Sulfo-NHS (product num. 56485) and BSA (product num. 9048-46-8) were from Sigma-Aldrich Japan. All of other chemical substances were purchased from Wako Pure Chemical Industries Ltd.

4. Flow-Cell System

For continuous and stable monitoring of the resonance frequency, the QCM cell was incorporated in the homebuilt flow-cell system. The temperature inside the cell was kept at 37± 0.02 ° C. The carrier fluid was PBS and the flow rate was 0.16 ml/min. We first monitored the fundamental resonance frequency near 54 MHz by the frequency-scan method. After the resonance frequency became stable with the frequency fluctuation smaller than 10^{-7}, we switched the measurement mode to the phase method to make a quicker measurement (∼0.1 s). The hIgG solution (PBS containing small amount of hIgG) was then injected, which was followed by the injection of glycine-HCl buffer (0.1 M, pH 2.2) for dissociating hIgG molecules from SPA, and by the injection of the carrier PBS. This injection sequence (PBS, hIgG, glycine-HCl, PBS, ⋯) was repeated with various hIgG concentrations.

5. Vibrational Analysis

Here, we investigate the availability of the Sauerbrey equation and the influence of the electrode layers on the frequency sensitivity when the crystal becomes thinner. The Sauerbrey equation[10] has been widely accepted and adopted to calculate the amount of adsorbed organic molecules from the resonance frequency change and to determine the kinetic constants. It indicates that the fractional frequency decrease ($\Delta f/f$) equals the ratio of the adsorbed mass

to the crystal mass. It gives almost correct answer when the mass of the adsorbed material is much smaller than that of the crystal, that is, when the QCM shows relatively lower sensitivity. When the crystal thickness decreases, however, the Sauerbrey equation tend to disagree with the exact answer because of the elastic-coupling effect among the crystal, electrode layers, and the adsorbed organic layer.[13)]

The resonance frequencies of a plane bulk wave in a layered-structure solid can be accurately calculated when the elastic constants, mass densities, and thicknesses of individual layers are known.[18,19)] Considering that the QCM tip consists of three layers, the crystal layer, the metallic electrode layer, and the organic-material layer, the frequency equation takes the form[18)]

$$\mu_{\mathrm{q}} k_{\mathrm{q}} \tan\eta - \mu_{\mathrm{e}} k_{\mathrm{e}} \tan(\gamma - \delta) = 0 \tag{1}$$

Here, δ is determined through

$$\cos\delta = \cos\alpha\cos\beta + p\sin\alpha\sin\beta$$

$$\sin\delta = \cos\alpha\sin\beta - p\sin\alpha\cos\beta$$

and

$$\alpha = k_{\mathrm{org}} d_{\mathrm{org}}, \beta = k_{\mathrm{e}} d_{\mathrm{org}}, \gamma = k_{\mathrm{e}}(d_{\mathrm{org}} + d_{\mathrm{e}}), \eta = k_{\mathrm{q}} d_{\mathrm{q}}, p = \frac{\mu_{\mathrm{org}} k_{\mathrm{org}}}{\mu_{\mathrm{e}} k_{\mathrm{e}}}$$

Where, μ and d denote the shear modulus and thickness, respectively. k is the wavenumber given by $k = 2\pi f \sqrt{\rho/\mu}$ with the mass density ρ. The subscripts q, e, and org express quantities of the crystal, the electrode layer, and the organic layer, respectively. We used d_{q}=30 μm, μ_{q}=29 GPa, ρ_{q}=2648 kg/m^3, μ_{e}=28 GPa, and ρ_{e}=19284 kg/m^3, which are standard values for an AT-cut quartz and gold. Concerning the properties of the organic-material layer, we assume an IgG layer with d_{org}=10 nm and the mass density 1500 kg/m^3, which are determined referring to the human IgG structure.[20,21)]

6. Results and Discussion

First, we show the significance of an electrodess QCM. Figure 2 shows the effect of the gold electrode on the fractional frequency change when a 10-nm thick IgG layer is added on the electrode surface. The shear modulus of the IgG layer was assumed to be 0.1, 1, and 10 MPa. Use of the metallic electrode decreases the amount of the frequency change. The electrodes of 300 nm on both sides, for example, lower the QCM sensitivity by 20% compared with the electrodeless case. The 9-nm thick gold film we used, however, affects little the sensitivity. Figure 2 also clarifies the important fact that the Sauerbrey equation tends to overestimate the frequency change as the electrode thickness increases. These unfavorable effects associated

with the electrode become more serious as the crystal becomes thinner. Thus, the electrodeless approach is the key for achieving a high-sensitive and quantitative QCM.

Next, we show enhanced sensitivity of our electrodeless QCM. Figure 3 shows frequency responses to the injections of the hIgG solutions detected by three electrodeless QCMs with thicknesses 30, 50, and 300 μm. (For comparison, we made the immunoassay measurement with 50 and 300 μm electrodeless QCMs.) The sensitivity to the hIgG detection obviously increases as the QCM becomes thinner. As demonstrated in Fig. 4, the 30-μm thick QCM clearly monitors the change of the resonance frequency responding to the injection of the hIgG solution with the concentration as low as 100 pg/mL: None of previous works succeeded in the real-time detection of hIgG-related reaction for such a low hIgG concentration. For example, Muramatsu et al.[5] monitored the hIgG-SPA reaction using a conventional 180-μm thick QCM and showed the binding curve for the 100 ng/mL IgG solution. Tang et al.[22] gave the binding curve between hIgG and anti-hIgG for a 45 ng/mL hIgG solution. Table 1 compares the frequency change observed by the present electrodeless QCM with those reported previously for the same IgG concentration. Our QCM achieves the highest sensitivity.

Finally, we discuss the kinetics of the binding reaction. When we use a flow-injection system, the frequency change during the binding reaction is expressed by[4]

$$\frac{\Delta f(t)}{f_0} = A\left\{e^{-(k_a C_{IgG} + k_d)t} - 1\right\} \tag{2}$$

Where $\Delta f(t) = f(t) - f_0$ is the frequency decrement caused by the binding reaction, and f_0 is the frequency before the reaction. k_a and k_d are the association and dissociation rate constants of their binding reaction, respectively. C_{IgG} represents the hIgG concentration in the QCM cell. A is a positive constant. Thus, this equation indicates that the frequency decrease obeys the exponential function. Figure 5 shows the logarithmic plot of the binding curve observed by the 30-μm thick electrodeless QCM for a 1-μg/mL hIgG solution, revealing that Eq.(2) completely fits to the measured frequency change. However, a single exponential curve failed to fit with the measurement for a 10-μg/mL hIgG solution: The binding curve appears to be fitted by two exponential curves as shown in Fig. 6, indicating that two sets of the kinetic constants, or two affinity constants, govern the reaction. Many researchers studied the binding behavior between IgG and SPA.[24–29] Their common conclusions include that Fc region of IgG molecule possesses two functional binding sites to protein A near the outer interfaces between C_H2 and C_H3 domains, and that protein A contains four monovalent binding sites to the Fc portion of IgG.[28] The molar ratio of IgG to protein A to construct a complex is one in larger protein A excess, and it approaches to two in larger IgG excess.[29] Therefore, both of two Fc sites can bind with the four monovalent sites of SPA when the number of the hIgG molecule is smaller. Therefore, the affinity will be higher at the beginning of the injection of the hIgG molecules, but it becomes lower because of the hindrance effect when the IgG concentration

is higher.

7. Conclusions

The high-frequency wireless-electrodeless QCM was developed as an immunosensor. The 30-μm thick AT-cut quartz plate was excited by the line antenna with the noncontacting manner, and its fundamental resonance frequency near 54 MHz was measured by the same antenna. The vibrational analysis for the multilayered oscillator quantified the influence of the gold electrodes on the resonance-frequency change when the target material was adsorbed on the surface, and it predicted that the QCM sensitivity significantly deteriorates when the gold electrodes were deposited. The homebuilt QCM method was used to detect human IgG through protein A immobilized on one surface of the crystal. It succeeded in the real-time monitoring of their binding reaction even for a solution containing very small amount of IgG with the concentration 100 pg/mL. The two-step binding reaction was observed in the 10-μg/mL hIgG solution.

References

1) M. Capurro, I. R. Wanless, M. Sherman, G. Deboer, W. Shi, E. Miyoshi, J. Filmus: Gastroenterology. **125** (2003) 89.

2) M. Forman, J. Trojanowski, and V. Lee: Nat. Med. **10** (2004) 1055.

3) M. J. Eddowes: Biosensors. **3** (1987) 1.

4) Y. Liu, X. Yu, R. Zhao, D. Shangguan, Z. Bo and G. Liu: Biosensors and Bioelectronics. **18** (2003) 1419.

5) H. Muramatsu, M. Dicks, E. Tamiya and I. Karube: Anal. Chem. **59** (1987) 2760.

6) N. Pan and J. Shih: Sensors and Actuators B. **98** (2004) 180.

7) C. Larsson, M. Rodahl and F. Hook: Anal. Chem. **75** (2003) 5080.

8) G. Stengel, F. Hook and W. Knoll: Anal. Chem. **77** (2005) 3709.

9) J. Park, S. Kurosawa, H. Aizawa, H. Hamano, Y. Harada, S. Asano, Y. Mizushima and M. Higaki: Biosensors and Bioelectronics. **22** (2006) 409.

10) G. Sauerbrey: Z. Phys. **155** (1959) 206.

11) H. Ogi, K. Wada and M. Hirao: Jpn. J. Appl. Phys. **43** (2004) 3024.

12) H. Ogi, K. Motohisa, T. Matsumoto, T. Mizugaki and M. Hirao: Biosensors and Bioelectronics. **21** (2006) 2001.

13) H. Ogi, K. Motohisa, T. Matsumoto, K. Hatanaka and M. Hirao: Anal. Chem. **78** (2006) 6903.

14) H. Ogi, H. Niho and M. Hirao: Appl. Phys. Lett. **88** (2006) 141110.

15) H. Ogi, T. Tada, J. Tian and M. Hirao: Jpn. J. Appl. Phys. **44** (2005) 4381.

16) H. Ogi, M. Hirao, T. Tada and J. Tian: Phys. Rev. B **73** (2006) 174107.

17) M. Hirao and H. Ogi, EMATs for Science and Industry: Noncontacting Ultrasound Measurements (Springer-Kluwer, Boston, 2003).

18) H. Ogi, G. Shimoike, M. Hirao, K. Takashima and Y. Higo: J. Appl. Phys. **91** (2002) 4857.

19) H. Ogi, Y. Tomiyama, Y. Shoji, T. Mizugaki and M. Hirao: Jpn. J. Appl. Phys. **45** (2006) 4678.

20) V. Sarma, E. Silverton, D. Davies, and W. Terry: J. Biol. Chem. **246** (1971) 3753.

21) F. Nollb, G. Lutscha, and H. Bielkab: Immunology Lett. **4** (1982) 117.

22) D. Tang, R. Yuan and Y. Chai: Biosensors and Bioelectronics. (2006) in press.

23) C. Zhou, J. Friedt, A. Angelova, K. Choi, W. Laureyn, F. Frederix, A. Francis, A. Campitelli, Y. Engelborghs, and G. Borghs, G: Langmuir **20** (2004) 5857.

24) G. Kronvall, P. Quie, and R. Williams: J. Immunol. **104** (1970) 273.

25) S. Kessler: J. Immunol. **115** (1975) 1617.

26) D. Lancet, D. Isenman, J. Sjödahl, J. Sjöquist and I. Pecht: Biochem. Biophys. Res. Commun. **85** (1978) 608.

27) E. O'Keefe and V. Bennett: J. Biol. Chem. **25** (1980) 561.

28) J. Deisenhofer : Biochem. **20** (1981) 2361.

29) D. Hanson and V. Schumaker: J. Immunol. **132** (1984) 1397.

Table I. Comparison of the QCM sensitivity for detecting 10 μg/mL IgG solution.

	QCM thickness (μm)	C_{IgG} (μg/mL)	recepter	Δf (Hz)	f_0 (MHz)	$\Delta f/f_0$ (10^{-5})
present	30	10	Protein A	10562	54	19.6
Muramatsu et al.[5]	180	10	Protein A	200	9	2.2
Pan and Shih[6]	180	10	C60-Anti-IgG	350	10	3.5
Zhou et al.[23]	300	11.5	ODT-SAM	18	5	0.36

Figure Caption

Fig. 1 Homebuilt QCM cell. The 30-μm thick AT-cut quartz was installed in the cell, which was excited by the line antenna embedded in the bottom-cell wall. The antenna consists of three straight lines; two for generation and detection of the shear vibration, and the other for grounding.

Fig. 2 Dependence of the amount of the resonance-frequency shift caused by the adsorption of the 10-nm thick IgG layer on the 30-μm thick AT-cut quartz on the gold-electrode thickness. Three IgG shear moduli, 0.1, 1, 10 MPa, were assumed. The results were obtained from Eq. (1). Dashed line shows the prediction by the Sauerbrey equation.

Fig. 3 Behavior of the frequency change observed by the three electrodeless QCMs responding to the injections of the hIgG solutions. The arrow indicates the arrival time of the hIgG solutions.

Fig. 4 The resonance-frequency change observed by the 30-μm thick electrodeless QCM when a 100 pg/mL hIgG solution was injected. Arrows indicate the arrival times of the solutions. G-HCl denotes the glycine-HCl solution.

Fig. 5 Logarithmic plot of the resonance-frequency change measured by the 30-μm thick electrodeless QCM when a 1 μg/mL hIgG solution was injected. The dashed straight line is the fitted function (Eq. (2)).

Fig. 6 The resonance-frequency change caused by the injection of a 10 μg/mL hIgG solution (solid line) and fitted exponential functions (dashed lines). The two-step binding reactions are suggested.

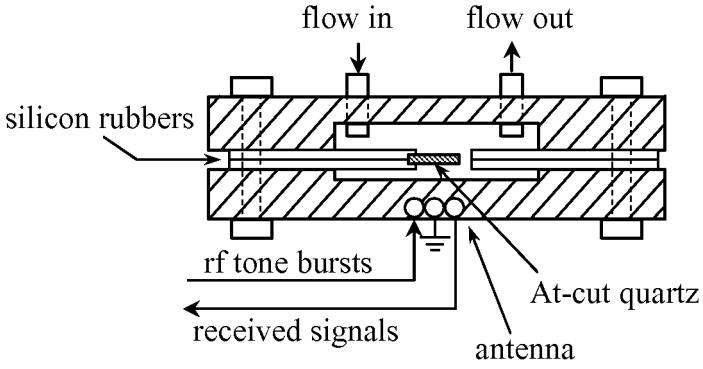
flow in
flow out
silicon rubbers
rf tone bursts
received signals
At-cut quartz
antenna

Fig. 1.

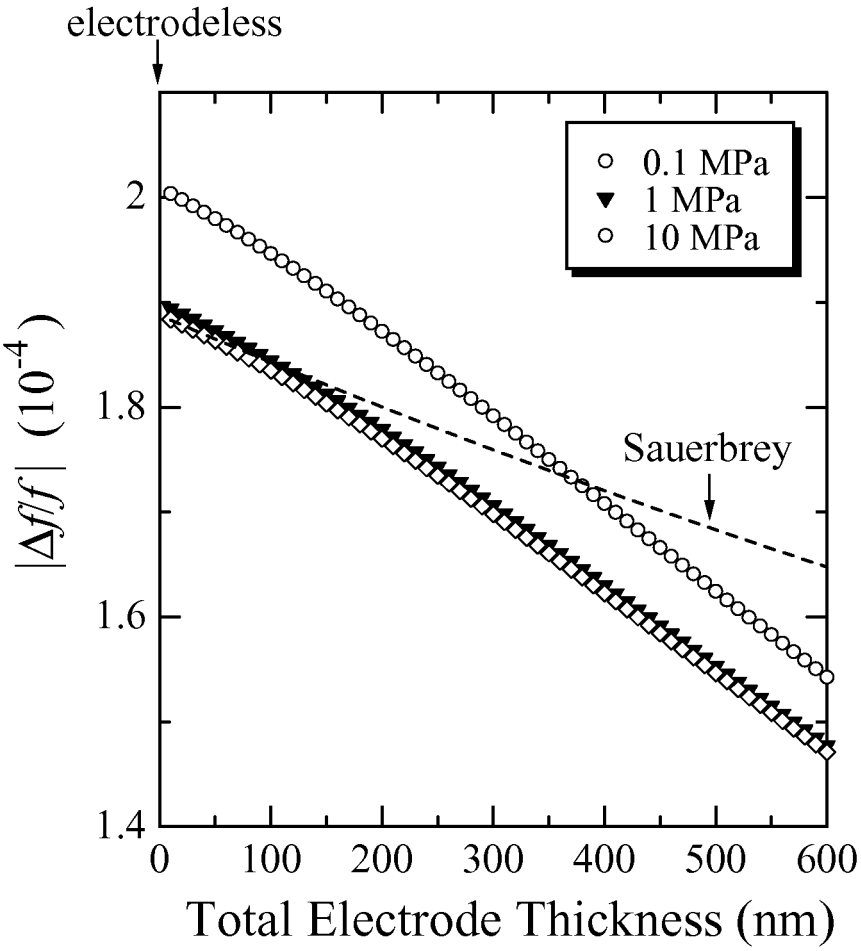
electrodeless
0.1 MPa
1 MPa
10 MPa
Sauerbrey
2
1.8
1.6
1.4
0
100
200
300
400
500
600
|Δf/f| (10^-4)
Total Electrode Thickness (nm)

Fig. 2.

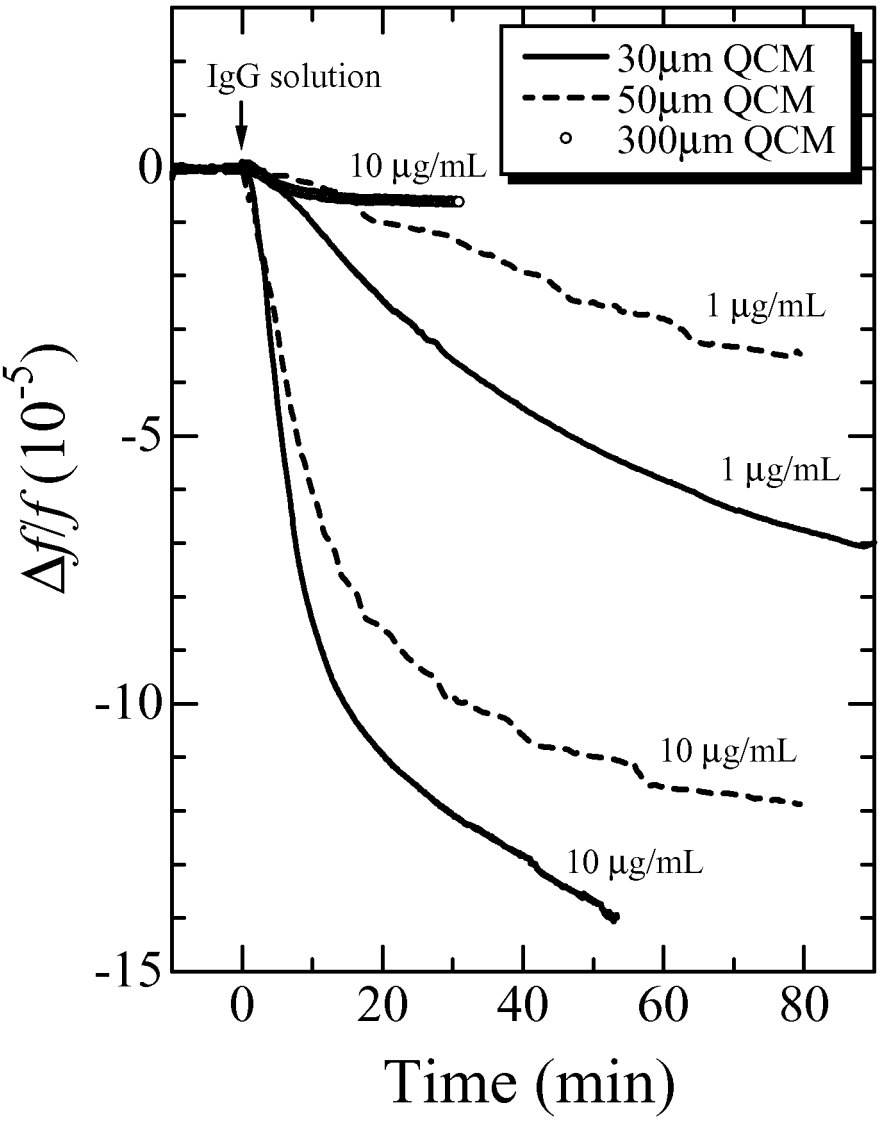
IgG solution
30μm QCM
50μm QCM
300μm QCM
10 μg/mL
1 μg/mL
1 μg/mL
10 μg/mL
10 μg/mL
0
-5
-10
-15
0
20
40
60
80
Δf/f (10^-5)
Time (min)

Fig. 3.

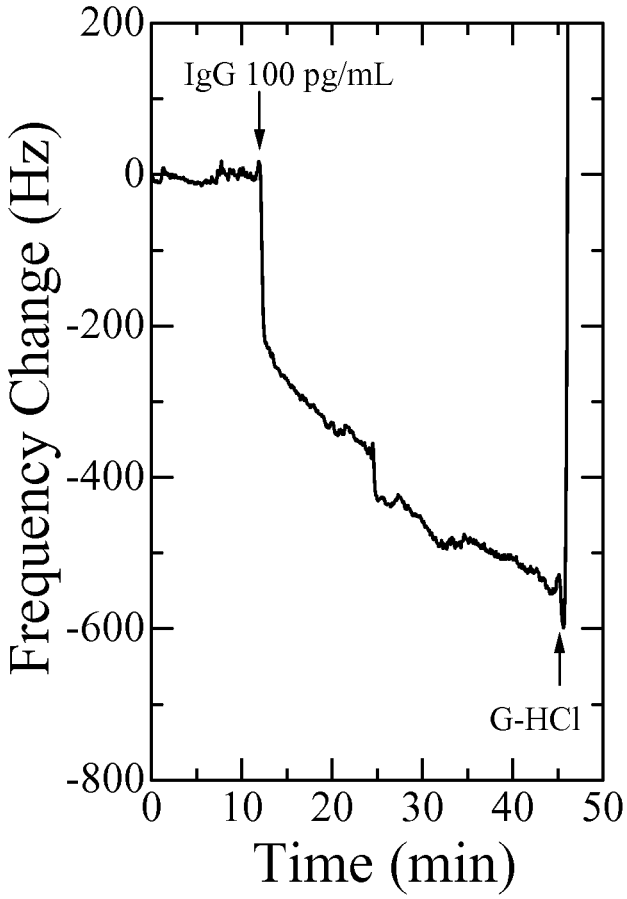
IgG 100 pg/mL
G-HCl
Frequency Change (Hz)
Time (min)
200
0
-200
-400
-600
-800
0
10
20
30
40
50

Fig. 4.

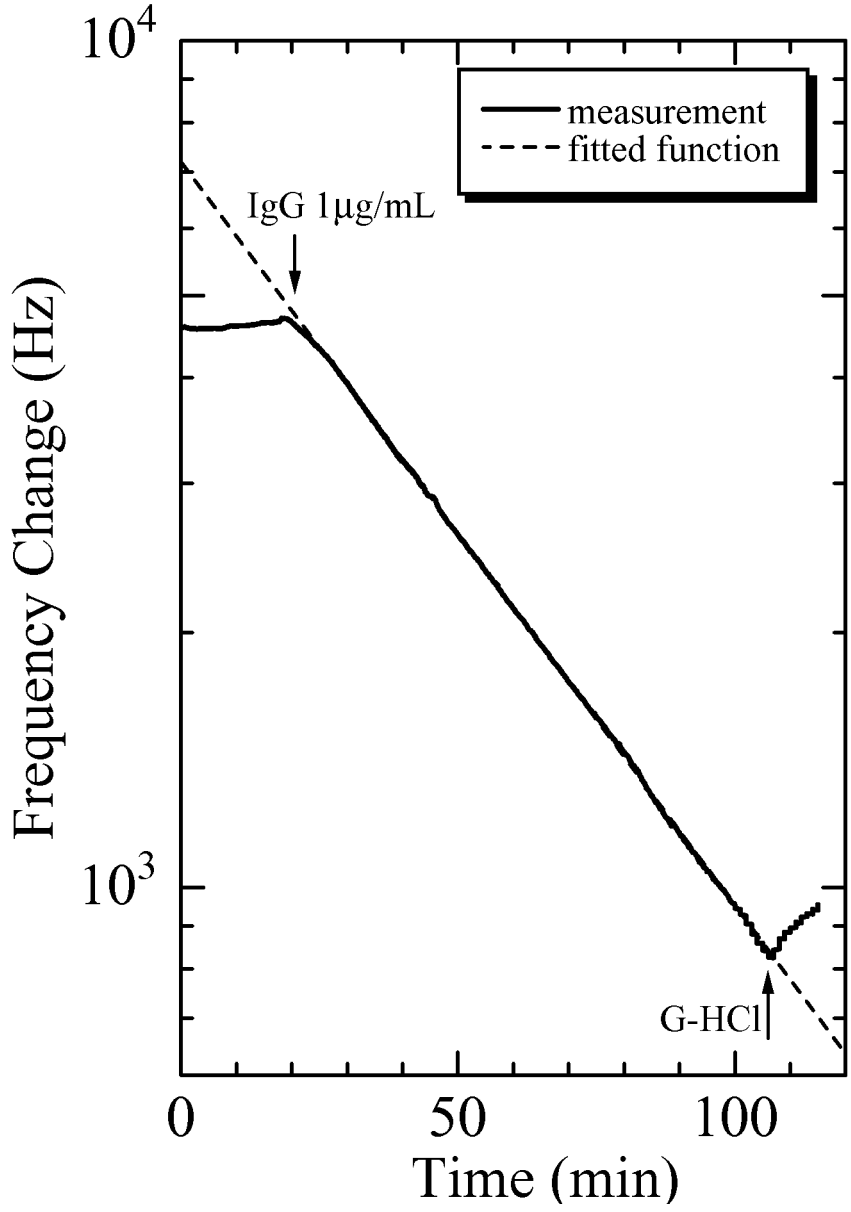
10^4
10^3
Frequency Change (Hz)
measurement
fitted function
IgG 1μg/mL
G-HCl
0
50
100
Time (min)

Fig. 5.

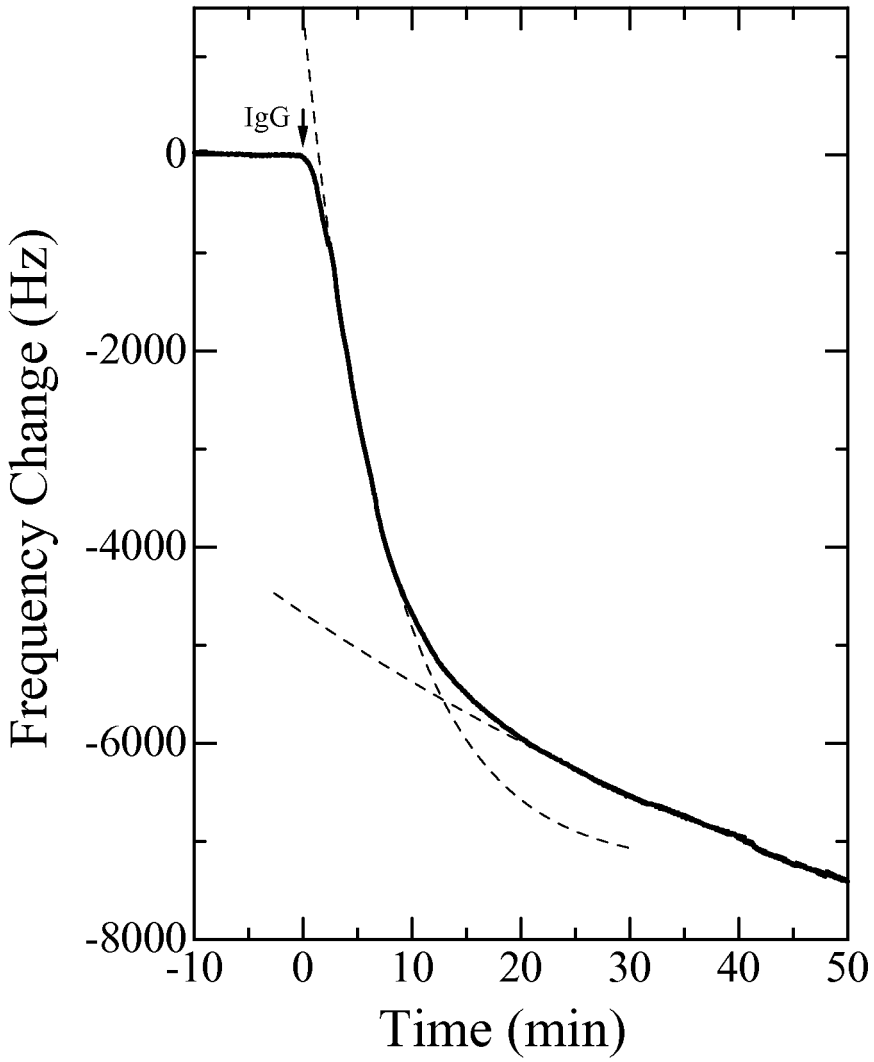
IgG
0
-2000
-4000
-6000
-8000
Frequency Change (Hz)
-10
0
10
20
30
40
50
Time (min)

Fig. 6.